Nitrogen transport in Coffs Creek over seasonal and flood scales

Coffs Harbour City Council Environmental Levy Program

Rebecca L. Woodrow; Praktan D. Wadnerkar; Shane A. White; Ceylena J. Holloway; Stephen R. Conrad; James P. Tucker; Kay L. Davis; Christian J. Sanders; Isaac R. Santos

January 2022

Southern Cross University
National Marine Science Centre

Prepared for: Coffs Harbour City Council

Citation: Woodrow, R. L., Wadnerkar, P. D., White, S. A., Holloway C. J., Conrad, S. R., Tucker, J. P., Davis K. L., Sanders, C. J., & Santos, I. R. (2022). Nitrogen transport in Coffs Creek over seasonal and flood scales. National Marine Science Centre, Southern Cross University, Coffs Harbour, NSW. 33 pages.

Contact:

Rebecca Woodrow

Phone: 0434616414

Email: rebecca.woodrow@scu.edu.au

Address: National Marine Science Centre

2 Bay Drive

Charlesworth Bay

Coffs Harbour, NSW

Australia, 2450

Acknowledgements: We acknowledge and pay respect to the people of the Gumbaynggirr Nation on whose Land we work, meet, and study. We recognise the significant role the past and future Elders play in the life of the University and the region. We are mindful that within and without the buildings, the Land always was and always will be Aboriginal Land.

This project was funded by the Coffs Harbour City Council's Environmental Levy program. We acknowledge the contributions of Samantha Hessey, Project Officer for the Orara River Rehabilitation Project & Regional State of the Environment Reporting, Coffs Harbour City Council for inspiring and supporting this project. This report belongs to the public domain. Original data is available at https://doi.pangaea.de/10.1594/PANGAEA.937740 (Woodrow, 2021).

Table of Contents

List of figures 4

List of tables 5

Executive Summary 6

1. Introduction 7

2. Materials and Methods 9

2.1 Study area 9

2.2 Monthly sampling and analysis 10

2.3 Flood sampling and analysis 11

2.4 Calculations 12

3. Results and discussion 13

3.1 Monthly observations 13

3.1.1 Hydrological conditions over an annual scale 13

3.1.2 Nitrogen species and dissolved organic carbon over an annual scale 15

3.2 Flood observations 18

3.2.1 Hydrological conditions over a flood scale 18

3.2.2 Nitrogen species and dissolved organic carbon over a flood scale 20

3.3 Annual and flood comparisons 25

4. Conclusion 28

5. Recommendations 29

6. References 30

List of figures

Figure 1. Map of sampling locations on the Coffs Creek estuary, NSW, Australia. Green dots indicate numbered seasonal sampling sites (S1 to S6), and the red dots indicate the upstream and downstream episodic time-series sampling sites. 10

Figure 2. Rainfall, soil moisture, and runoff over the period of July 2017 to June 2018 and distribution of monthly samples of salinity, dissolved oxygen (DO), and nitrate + nitrite (NO_X) in Coffs Creek estuary, Australia. Data were interpolated in SigmaPlot 13.0 using monthly spatial near-surface observations. 15

Figure 3. (A) Near-surface dissolved organic carbon (DOC), (B) total dissolved nitrogen (TDN), (C) nitrate + nitrite (NO_X) patterns of linear reduction, and (D) ammonium (NH_4^+) pattern of linear increase from the upper estuary to the lower estuary in Coffs Creek, Australia. Data points are annuals with error bars representing intra-annual variance (calculated as SE). 16

Figure 4. Time-series observations of hourly rainfall and water chemistry parameters collected over two hundred and thirty-two hours (3rd to 13th March 2018). The left stack shows all of the samples, while the right stack zooms in two tidal cycles. The green shading indicates a removal of nitrogen between the upstream and downstream stations, while the red shading indicates an addition of nitrogen. The scale of the nitrate removal is much larger than the DON and ammonium addition (Wadnerkar et al., 2019). 21

Figure 5. Nitrogen species (NH_4^+, NO_x, and DON) pre-, during, and post-rain at the upstream and downstream time series stations (Wadnerkar et al., 2019). 23

Figure 6. Scatter plots of salinity versus NOx concentration and NOx concentration versus NH_4^+ and DON (pre-, during, and post-rain, as well as during the individual precipitation events (Wadnerkar et al., 2019). 24

Figure 7. Bar chart showing the percent retention of the Coffs Creek estuary (NO_x and TDN) (Wadnerkar et al., 2019). 24

Figure 8. Nitrogen loads of surface water from upstream and downstream time-series stations. Note the different scales for NO_X, NH_4^+, and DON (Wadnerkar et al., 2019). 25

Figure 9. NO_X concentrations in Coffs Creek estuary over annual scales and at peak flood conditions. White circles represent monthly surveys upstream and black circles represent monthly surveys downstream. The white triangle represents peak flood observation upstream, and the black triangle represents peak flood observation downstream. Only low tide time-series observations were utilised to reduce tidal bias. In March, the monthly NO_X observation was taken six days after the rain-event N_2O observation. The increase in NO_X captured during the rain event is the difference between the spatial March observation and the peak flood observation. 26

Figure 10. Comparison of NO_X loads upstream and downstream of Coffs Creek estuary in dry, wet, and flood conditions. Error bars are standard error. 27

Figure 11. Monthly (A) NO_X concentration versus runoff, (B) NO_X concentration versus soil moisture and flood (C) NO_X concentration versus runoff, (D) NO_X concentration versus soil moisture. Linear trendlines indicate a steady increase in runoff over the flood event while the exponential trendlines indicate a sharp and rapid increase in NO_X concentrations during the flood. 28

List of tables

Table 1. In-study, site-specific measurements in Coffs Creek estuary, Australia, showing the distance of each sampling site from the estuary mouth, the surface area of each site, percentage total surface area each site contributes to the total estuary, and the mangrove density. 12

Table 2. Summary table of the annual average ± SE, and range of estuarine physicochemical and nutrient parameters for each of the Survey Sites 1-6 of Coffs Creek estuary, Australia. 14

Table 3. Daily rainfall, runoff, and soil moisture values for each of the eight periods before, during, and after the episodic rain event in Coffs Creek estuary, NSW, Australia (BOM, 2021a, 2021b). 19

Executive Summary

Nitrogen (N) escaping agricultural and urban lands can reduce water quality in downstream estuaries and the coastal ocean. As part of Coffs Harbour City Council's Environmental Levy grant program, Southern Cross University performed water quality investigations in Coffs Creek, NSW, Australia, to examine N transport along the estuary and into the Solitary Islands Marine Park (SIMP). We used new and existing data to assess water quality along Coffs Creek, quantifying N concentrations and estimating the N attenuation capacity of the estuary over 12 months and during a minor flood event. Intensive horticulture is a source of N (in the form of NO_X) to Coffs Creek due to land use in the upper catchment area. Mean NO_X (nitrate plus nitrite) concentrations measured over an annual cycle were 5-fold over the Australia and New Zealand Environment and Conservation Council trigger values (ANZECC), and up to 14-fold over ANZECC after rainfall. Mean downstream ammonium (NH_4^+) concentrations were 7-fold over ANZECC.

Upper estuary NO_X loads were ~ 109 ± 82 kg NO_X km^{-2} $year^{-1}$. High NO_X attenuation (~ 81%) occurred instream, reducing exports to the SIMP (~ 18 ± 12 kg NO_X km^{-2} $year^{-1}$). In contrast, upper estuary NH_4^+ loads were ~ 3 ± 1 kg NH_4^+ km^{-2} $year^{-1}$. Overall, NO_X was the main form of dissolved inorganic nitrogen (DIN) at the most upstream site (~ 90%), while ammonium (NH_4^+) was the main form of DIN at the most downstream site (~ 75%). It is likely that either conversion of NO_X to NH_4^+ occurred instream or there were added NH_4^+ sources along the creek, increasing exports to the SIMP (~ 22 ± 11 kg NH_4^+ km^{-2} $year^{-1}$).

During a minor flood, NO_X was the main form of DIN at both upstream (~ 98%) and downstream sites (~ 77%). Mean upstream NO_X was 16-fold over ANZECC, peaking at 33-fold over ANZECC, whilst mean downstream NO_X was 9-fold over ANZECC, peaking at 43-fold over ANZECC.

High NO_X attenuation (71%) occurred during the initial day of the rain event. However, as NO_X loads increased during the flood, instream attenuation was reduced. Downstream NO_X loads peaked 48 hrs later with attenuation reduced to 20% from upstream inputs.

Low concentrations of NO_X (~ 5 µg L^{-1}) were found through the mangrove-dense middle of the estuary over the year in dry conditions. However, during the flood event, these concentrations increased 30-fold (~ 150 µg L^{-1}). This highlights the importance of nitrogen cycling and nitrogen load reduction capability within mangrove ecosystems and how this reduction capacity is overwhelmed during floods.

Our results highlight that mangrove-dominated creeks have a great capacity to filter out NO_X during dry through to moderately wet conditions. As a result, only the upstream waters of the creek are polluted by nitrogen during non-rain periods. However, during episodic rain events of increased

runoff and soil moisture, high loads of NO_X are exported downstream and overwhelm natural instream attenuation processes. As a result, the entire creek becomes polluted with nitrogen following large rain events.

1. Introduction

With funding from the Environmental Levy Grants program, Southern Cross University has performed nitrogen investigations along Coffs Creek estuary, NSW, Australia. This project complements our previous research in Double Crossing Creek, upstream of Hearnes Lake estuary, addressing water quality and nitrogen (N) attenuation capacity in Hearnes Lake catchment (Conrad et al., 2018, 2020; White et al., 2018, 2020).

The N loads found in Double Crossing Creek in 2018 were some of the highest ever recorded in a natural waterway on the east coast of Australia (White et al., 2018). NO_X concentrations were ~ 5000-fold the ANZECC water quality guidelines upstream and ~ 17-fold the ANZECC guidelines downstream (Australia and New Zealand Environment and Conservation Council, 2000; White et al., 2020).

Precipitation fluctuations due to climate change are predicted to have a substantial impact on riverine nitrogen loadings (Sinha et al., 2017). Increased precipitation frequency/intensity and more intensive land use will likely increase N mobilization and reduce downstream water quality. Estuarine ecosystems in agricultural and urbanised catchments are sensitive to intensified nutrient loading from anthropogenic sources. Nutrients are stored in the soil during dry conditions (Post et al., 1985), but rainfall mobilizes these nutrients deposited within the uppermost soil layers via surface runoff (Herbeck et al., 2011; Santos et al., 2013; White et al., 2018). As a result, heavy rainfall can flush nutrients from catchments to estuaries and finally, the ocean (Eyre, 2000; Kaushal et al., 2011; Wang et al., 2010; Maher et al., 2015).

However, estuaries can attenuate the flux of nitrogen (N) from land to the ocean, behaving as filters that remove nitrate through transformations to N gases (Masselink & Gehrels, 2015; White et al., 2021b). The common estuarine potential loss pathways for N are denitrification ($NO_3^- \rightarrow NO_2^- \rightarrow NO \rightarrow N_2O \rightarrow N_2$) and nitrification ($NH_4^+ \rightarrow NH_2OH$ [+ N_2O] $\rightarrow NO_2^- \rightarrow NO_3^-$). Estuarine N transforms through microbial metabolism that is often related to temperature and carbon availability (Wrage et al., 2001; Butterbach-Bahl et al., 2013).

Coastal intertidal wetlands such as mangroves and saltmarshes often fringe tidal estuaries such as Coffs Creek. These wetlands are highly productive and can remove large amounts of nutrients (Alongi, 2002) through sedimentation, filtration, microbial activity, and plant uptake (Mitsch et al., 2012; Sanders et al., 2016). Mangroves have an essential role in estuarine nitrogen cycling as they are highly productive systems with organic rich sediments and abundant crab burrows which drive porewater exchange and nitrogen processing within sediments (Tait et al., 2017). Furthermore, mangroves can efficiently regulate elevated inorganic nitrogen concentrations through denitrification (Rosentreter et al., 2021).

While mangroves are known to remove nitrogen (Reef et al., 2010), few investigations have quantified their efficiency at the ecosystem scale (Adyel et al., 2016; Jordan et al., 2011; Mitsch et al., 2005), particularly during major rain events that may transport much of the annual nitrogen loads to the ocean on short time scales (Santos et al., 2013; Scott et al., 2014; Wang et al., 2016). Episodic events, such as flooding, have the potential to disrupt ecological and biogeochemical processes (Alongi, 2002; Wadnerkar et al., 2019, White et al., 2021a). Investigations in nearby Double Crossing Creek found significant instream attenuation of NO_X loads during dry to moderately wet conditions. However, observations during a flood in the same creek found that instream processes were overwhelmed, and NO_X attenuation was significantly reduced (White et al., 2020).

Recent studies have investigated the influence of flow on rates of NO_X removal through natural creek attenuation (Wong et al., 2018; Wadnerkar et al., 2021) and the influence of soil saturation on N mobilisation (White et al., 2021). However, further research into how NO_X responds to rain events in sub-tropical estuaries is required to understand how N loading affects creek attenuation capacity in the semi-urbanised mixed-use catchment of Coffs Creek, NSW, Australia.

Here, we quantify the transport of nutrients within Coffs Creek estuary over seasonal and minor-flood scales. We focus on the flood to evaluate the potential for nitrogen attenuation before, during and after a large rain event. We build on earlier work by reporting detailed seasonal surveys and time-series observations during episodic events at a much greater spatial and temporal resolutions. We describe longitudinal monthly surveys performed along Coffs Creek estuary on eleven occasions over twelve months. Further, field investigations to capture an episodic rain event (flood) were conducted at upstream and downstream sites within Coffs Creek estuary using a time-series approach over eight days. Observations were performed during a dry period and over a minor flood event to investigate the drivers and loads of N within the creek. Specifically, we quantify N concentrations and loads along with the natural attenuation capacity of the creek (the removal of N) during both dry and wet conditions.

Our analyses include:

1) A comparison of the observed N concentrations over twelve months and during a minor flood event to Australia and New Zealand Environment and Conservation Council (ANZECC) water quality guidelines for lowland streams and estuaries in NSW.

2) A comparison of N loads along the creek transects, focusing on the upper and lower estuary.

3) Estimates of the attenuation capacity of Coffs Creek estuary N loads over twelve months and during a minor flood event.

To achieve these objectives, we rely on time series observations from a rain event previously published by Wadnerkar et al. (2019) and new seasonal surveys along the estuary, published by Woodrow et al. (2021) and part of an SCU Honours thesis by Rebecca Woodrow.

2. Materials and Methods

2.1 Study area

The study was performed in Coffs Creek estuary (30.30 °S, 153.10 °E) in Coffs Harbour, NSW, Australia (Figure 1). Coffs Creek is a 6 km long tidal estuary averaging 40 m in width and 0.6 m in depth, with a catchment area spanning ~ 25 km^2, and a mean water surface area of ~ 0.27 km^2. The mid and lower sections of the estuary contain ~ 0.19 km^2 of fringing mangroves with a general trend of recent sediment accretion in the first 4.5 km from the mouth (Conrad et al., 2017). The estuarine portion of Coffs Creek forms part of the SIMP. Approximately 18,000 people live in the catchment area (Coffs Harbour City Council, 2020). Land uses in the catchment area are 35% urban development, 23% horticultural, 12% forest, 11% recreational area 10% grazing, and 9% industrial (Coffs Harbour City Council, 2020). Horticulture is a significant source of nutrients to local waterways (White et al., 2018). Treated local urban wastewater is redistributed through oceanic channels, meaning there are no contributing sewerage treatment plant outfalls within Coffs Creek estuary (Reading et al., 2020).

Water quality within the estuary is considered poor-moderate due to high turbidity, high chlorophyll-a, low dissolved oxygen saturations, and nutrient sources in the upper catchment (Coffs Harbour City Council, 2020). Previous studies carried out in mangrove sediments of Coffs Creek revealed that heavy metal and nutrient accumulation was 2.5 times higher in recent sediments than in the 1950s (Conrad et al., 2017). The estuary acts as a sink for nitrate and N_2O in dry conditions due to nitrate consumption and shallow pore water exchange in mangrove sediments (Reading et al., 2017; Reading

et al., 2020). High tidally driven pore water exchange has been observed in the mangrove-fringed section of the estuary (Sadat-Noori et al., 2017).

This subtropical region receives ~ 1700 mm of annual precipitation and is mostly subject to episodic rather than seasonal rainfall patterns (Australian Government Bureau of Meteorology [BOM], 2021b). In the last decade, annual observations revealed a mean of 89, 34 and 15-days year^{-1} with ≥ 1, ≥ 10 and, ≥ 25 mm day^{-1}, rainfall, respectively (BOM, 2021b). Like many catchments on the east coast of Australia, the Coffs Creek hydrology is strongly influenced by episodic rainfall (BMT WBM, 2011). For example, in 2009, a storm resulted in flash flooding after 500 mm of rain within 48 hours (BMT WBM, 2011).

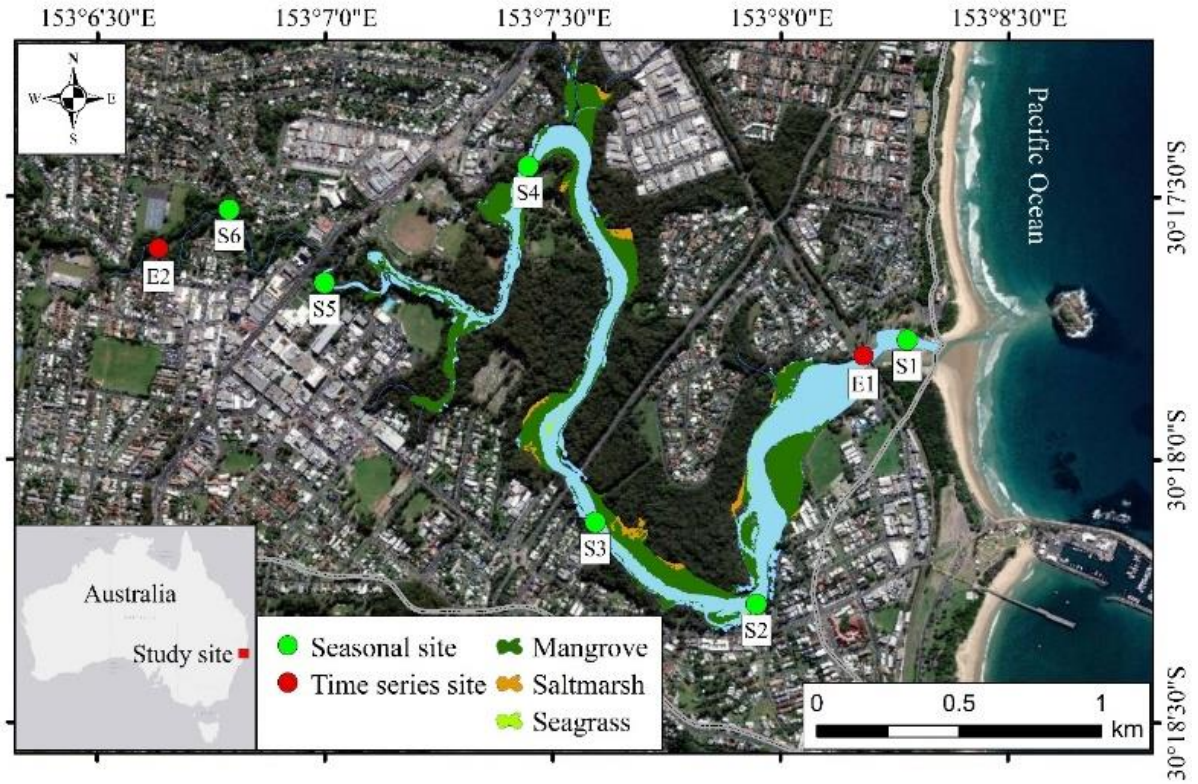

Figure 1. Map of sampling locations on the Coffs Creek estuary, NSW, Australia. Green dots indicate numbered seasonal sampling sites (S1 to S6), and the red dots indicate the upstream and downstream episodic time-series sampling sites.

2.2 Monthly sampling and analysis

Longitudinal monthly surveys were performed on eleven occasions from July 2017 to June 2018. A total of 66 samples were collected over a total period of 12 months. Water parameters (salinity, dissolved oxygen (DO), and temperature), nutrient, and gas samples were taken approximately every month (excluding September 2017) from the upper water column at 6 sites along the creek salinity gradient at low tide, from the estuary's mouth and to the upper freshwater creek (Figure 1). Samples

were also taken at the bottom of the water column at the halocline stratified sites (Sites 2-5). A calibrated YSI EC300A was used to measure salinity (± 0.02), whilst a calibrated Hach HQ40D measured DO (± 0.2 mg L^{-1}) and water temperature (± 0.10°C).

Nutrient samples (including duplicates), filtered and unfiltered, were collected with a sample-rinsed 60 mL polyethylene syringe. Samples for dissolved organic carbon (DOC) analysis were filtered using pre-combusted 0.7 µm GF/F filters (Whatman), into 40 mL borosilicate vials (USP Type I). Samples for nitrogen were immediately filtered using Satourious™ 0.45µm cellulose acetate syringe filters into 10 mL polyethylene sample tube. All samples were kept in a cold icebox, away from light, for less than 5 hr and then frozen until laboratory analysis. Analysis of DOC was performed with the 40 mL borosilicate vials (USP Type I) first treated with 30 µL of H_3PO_4 before analysis using an Aurora 1030W TOC Analyser (Thermo Fisher Scientific, ConFLo IV). Nutrient analysis of ammonium (NH_4^+), NO_x (nitrate plus nitrite), and total dissolved nitrogen (TDN) were performed on the 10 mL polyethylene sample tubes colourimetrically using a Lachat Flow Injection Analyser. Particulate nitrogen was not investigated because nitrate is well known to be the main nitrogen species in the study region even during rain events. (White et al., 2018; White et al., 2020). Analytical errors were calculated as the average coefficient of variation of replicates.

2.3 Flood sampling and analysis

Field investigations to capture an episodic rain event (flood) were conducted using a time-series approach between the 3rd and the 13th of March 2018. Observations began at the time-series sites upstream (< 100 m from the seasonal spatial survey Site 6), and near the estuary mouth (< 100 m from seasonal spatial survey Site 1) (Figure 2), 4 days prior to a predicted large rain event. The rain event (64.6 mm on the7th March 2018) spanned 24 hrs and then 6 additional days of measurements were taken with some intermittent minor rain events (22.4 mm between the 9th and 11th March 2018) during that period. Samples were collected at hourly intervals during intense rainfall and at three hourly intervals before and after the intense rainfall over a total period of two hundred and thirty-two hours.

At the downstream time-series station, a calibrated Hydrolab MS5 sonde measured and logged water temperature (± 0.02°C), DO (± 0.2 mg L^{-1}), and salinity (± 0.02) at 30 m intervals and a depth logger (CTD diver) measured water depth in 1-minute intervals. Discrete measurements for DO and pH at the upstream station were performed using a Hach multimeter (40 HQd, Hach, USA). Nutrient samples were collected and analysed as in the spatial surveys. The results of these observations were originally reported in Wadnerkar et al. (2019).

2.4 Calculations

Wind speed and rainfall data were retrieved from Coffs Harbour Airport station, 059151 (BOM, 2021b). Runoff and soil moisture data were obtained from the Australian Landscape Water Balance model (AWRA-L) (BOM, 2021a). The AWRA-L model is a grid-based distributed water balance model conceptualised for small catchments that is a function of streamflow observations, soil moisture and evapotranspiration. The flushing time was defined as the time required for incoming fresh water to replace the entire estuary volume (Eyre, 1997). Discharge ($m^3\ s^{-1}$) was calculated by multiplying the runoff ($m\ s^{-1}$) by catchment area (m^2). ArcGIS was used to estimate the catchment areas for discharge calculations, as well as the estuary surface areas of the 6 measured sections of the estuary to calculate mangrove density (Table 1).

Table 1. In-study, site-specific measurements in Coffs Creek estuary, Australia, showing the distance of each sampling site from the estuary mouth, the surface area of each site, percentage total surface area each site contributes to the total estuary, and the mangrove density.

	Site 1	**Site 2**	**Site 3**	**Site 4**	**Site 5**	**Site 6**
Distance from estuary mouth (km)	0.130	1.510	2.225	3.956	5.230	6.117
Surface area of fringe mangroves (%)	21	52	59	61	33	0
Surface area of estuary (km^2)	0.094	0.117	0.100	0.138	0.023	0.007
% of total surface area of estuary	20	24	21	29	5	1

N loads were estimated from the freshwater creek to the estuary, and from the estuary to the ocean. The difference between these two N loads was interpreted as either a nutrient sink or source within the estuary. The freshwater N concentration (C_{up}) was measured at the upstream time-series station that was not influenced by tides. The estuarine N concentration (C*) was calculated using the standard estuarine model widely used to estimate loads from estuaries to the ocean (Emerson et al., 1984; Santos et al., 2008). In the model, the nutrient/salinity relationships are extrapolated back to zero salinity (Y-axis intercept) to determine the effective N concentration prior to discharge into the ocean. The respective freshwater (C_{up}) and estuarine (C*) concentrations were then multiplied by the freshwater flow to estimate loads from the creek to estuary and from estuary to the ocean. Attenuation was then obtained by dividing the nutrient mass removed per day by the catchment area (24.5 km^2), mangrove area (0.19 km^2) and estuary surface area (0.27 km^2). The flushing time was defined as the

time required for imported fresh water to replace the total volume of the estuary (Eyre, 1997). The load (flux per area, per time) of NO_X and NH_4^+ were calculated using the equation:

$$\boldsymbol{F = C m Q / A}$$

where **F** is the flux of nutrients (g km^{-2} day^{-1}), **C** is the concentration of NO_X or NH_4^+ (µM), ***m*** is the molecular weight of the element (g per mol), **Q** is discharge (m^3 d^{-1}), and **A** is catchment area (m^2), unit conversions were used where appropriate.

We report mean ± standard error (SE) unless otherwise specified. Linear regression equations and r^2 values were calculated, with r^2 values evaluated using Pearson's correlation table with 2 degrees of freedom.

3. Results and discussion

3.1 Monthly observations

3.1.1 Hydrological conditions over an annual scale

The first 3 months of the seasonal surveys were dry, with soil moisture steadily dropping from 61% (month) to a low of 14% (month) (Figure 2). From July to October 2017, the total rainfall was 8.2mm, with most of that rainfall occurring on one day in the 3 months, (16th July, 6.8 mm). An 82.6 mm rain event occurred from the 1st – 4th October 2017, coinciding with a survey on the 4th of October, however data from the AWRA-L model showed little runoff was produced from this rain event. Soil moisture rose from 14% to 84% between 1st October and 17th October 2017, with a sharp increase following a 169.4mm rainfall event from the 12th – 17th October 2017. Isolated minor episodic rain events occurred between November and February, with no rain or runoff seven days prior to our observations in those months. On 3rd – 13th March 2018, a 94.9 mm rain event was captured with detailed sampling (see section 3.2). Heavy rainfall and flash flooding was predicted four days before we started our flood observations. On 7th of March 2018, the creek level increased from 0.8 m to 1.1 m at high tide and from 0.09 to 0.6 m at low tide following 64.6 mm of rainfall (BOM, 2021b).

Water temperatures ranged from 15.1°C to 30.2°C over the year across all sites, following seasonal patterns, with the highest temperatures recorded at Sites 2 and 3 (30.2°C) during February 2018, and the lowest temperature upstream at Site 6 (15.1°C) in August 2017 (Table 2; Appendix A). Salinity followed a predictable trend with a lower mean value at the upper estuary (Site 6; 4 ± 1.9) near the freshwater source and a higher mean value near the ocean (Site 1; 30.3 ± 1.4). The high rainfall prior to the July observation, and in March and June reduced salinity down through the estuary (Site 1; 25.7 ± 3.8). Dry conditions from November to February coincided with higher salinity values (18.3) in the

upper estuary and the lower estuary (35). Dissolved oxygen (DO) was mostly under-saturated (75.7 ± 2.9%) over the year with DO typically higher at the estuary mouth at Site 1 (99.2 ± 3.3% sat.), and lower upstream at Site 6 (73.1 ± 6.1% sat.) (Figure 3). Pockets of low DO were observed in the upper estuary in dry conditions, with annual lows at Site 5 in October (5.3% sat.) and February (16% sat.). The low oxygen conditions penetrated along the estuary through the areas of high mangrove density (Sites 2, 3, and 4) in October as soil moisture dropped to saturation lows of 22%, consistent with higher salinity infiltrating the upper estuary (annual high of 28.8% sat. at Site 5).

Table 2. Summary table of the annual average ± SE, and range of estuarine physicochemical and nutrient parameters for each of the Survey Sites 1-6 of Coffs Creek estuary, Australia.

	Annual average and standard error **Annual min - max**					
	Site 1	**Site 2**	**Site 3**	**Site 4**	**Site 5**	**Site 6**
Temperature (˚C)	22.3 ± 1.1 17.6 - 28	22.6 ± 1.2 15.9 - 30.2	22.8 ± 1.2 16.5 - 30.2	23.3 ± 1 17.1 - 28.8	22.8 ± 1.3 16.1 -27.8	20.9 ± 1.3 15.1 - 27.4
DO (% sat.)	99.2 ± 3.3 76.3 - 115	84.2 ± 2.8 63.8 - 97.5	80.9 ± 3.9 60.2 - 98.2	69.4 ± 6.6 15.9 - 97.5	47.8 ± 7.9 16 - 82.1	73.1 ± 6.1 34.6 - 101.3
Salinity	30.3 ± 1.4 18.1 - 35	27.1 ± 1.9 15.4 - 33.3	24.7 ± 2.5 3.5 - 32.3	21.1 ± 2.8 4.6 -32.4	14.4 ± 2.9 0.9 - 28.8	3.9 ± 1.9 0.1 - 18.3
DOC (µM)	108 ± 8.50 67 - 156	162 ± 15.0 77 - 244	196 ± 19.6 111 -290	241 ± 34.9 106 - 345	322 ± 40.9 157 - 603	440 ± 45.1 161 - 607
TDN (µM)	13.8 ± 1.9 7.4 - 30.5	17.4 ± 3.1 7.3 - 38.9	16.5 ± 2.4 7.6 - 33.5	20.9 ± 4.1 10.6 - 57.1	22.1 ± 3.5 8.6 - 46.8	25.3 ± 4.1 8.2 - 53.1
NH_4^+ (µM)	7.1 ± 0.50 4.6 - 9.5	6.2 ± 0.60 4.1 - 11.7	5.4 ± 0.80 2.5 - 13.1	5.5 ± 1.20 2.2 - 14.8	4.9 ± 1.10 2.3 - 15.3	1.6 ± 0.60 0.0 - 7.2
NO_X (µM)	2.4 ± 0.9 0.0 - 8.4	4.7 ± 2.30 0.0 - 24.1	5.4 ± 2.50 0.0 - 24.1	6.9 ± 3.60 0.0 - 34.4	12.1 ± 4.6 0.0 - 38.5	14.4 ± 4.7 0.1 - 42.5

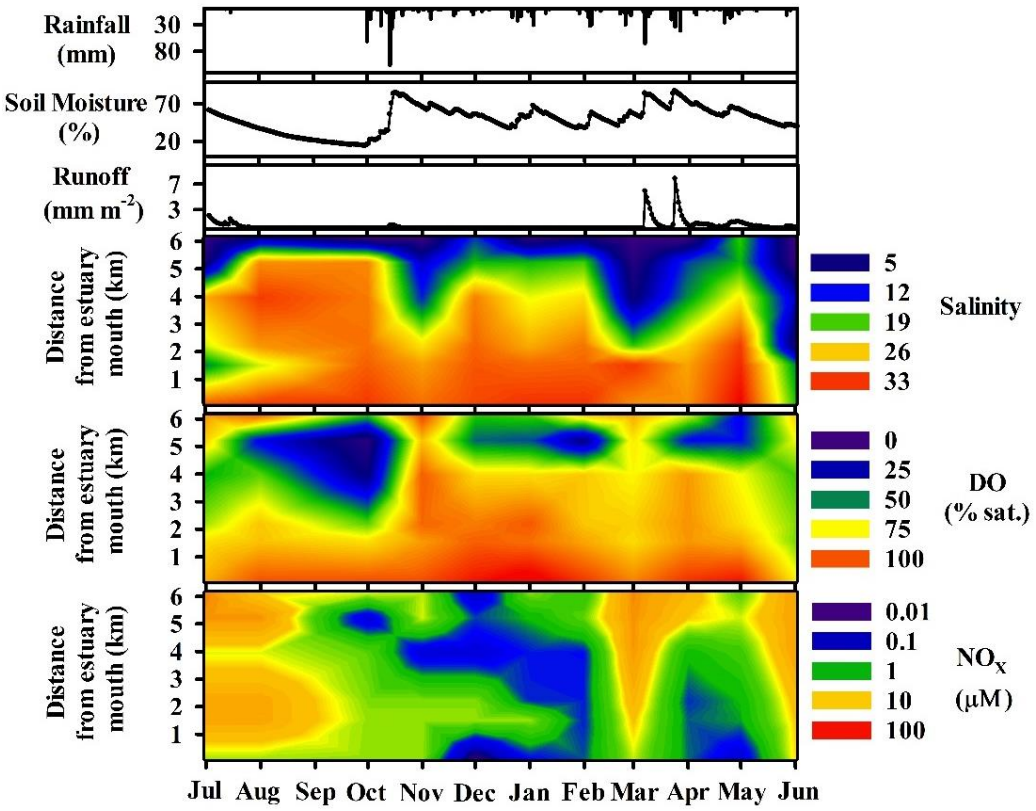

Figure 2. Rainfall, soil moisture, and runoff over the period of July 2017 to June 2018 and distribution of monthly samples of salinity, dissolved oxygen (DO), and nitrate + nitrite (NO_X) in Coffs Creek estuary, Australia. Data were interpolated in SigmaPlot 13.0 using monthly spatial near-surface observations.

3.1.2 Nitrogen species and dissolved organic carbon over an annual scale

Annual average DOC concentrations were 440 ± 45 µM in the upper estuary (Site 6), following a linear reduction ($r^2 = 0.95$, $p < 0.01$) down to 107.5 ± 8.5 µM near the mouth of the estuary (Site 1) (Figure 3A). A linear pattern of reduction also occurred with the annual average of TDN ($r^2 = 0.95$, $p < 0.01$) from 25.3 ± 4.1 µM upstream (Site 6) to 13.8 ± 1.9 µM downstream (Site 1) (Figure 3B). Coffs Creek estuary was found to be a hot spot of nitrogen (TDN) in this study over the year and strongly agreed with previous investigations of 23.6 ± 2.4 µM (Reading et al., 2017).

DIN made up ~ 63% of the TDN in the upper estuary (Site 6) over the 11 sampling campaigns, with NO_X contributing ~ 90% of DIN. DIN made up ~ 68% of the TDN in the lower estuary (Site 1), with NH_4^+ contributing ~ 75% of DIN. Annual average NO_X concentrations at Site 6 (upstream) were ~ 7-fold higher than Site 1 (downstream) with concentrations of 14.4 ± 4.7 µM (Site 6) linearly decreasing ($r^2 = 0.94$, $p < 0.01$) to 2.4 ± 0.9 µM (Site 1) (Figure 3C). Annual average NH_4^+ showed an opposite trend to TDN and NO_X with a 4-fold linear increase from the upper estuary to the lower estuary ($r^2 = 0.76$, $p < 0.05$) from 1.6 ± 0.6 µM (Site 6) to 7.1 ± 0.5 µM (Site 1) (Figure 3D).

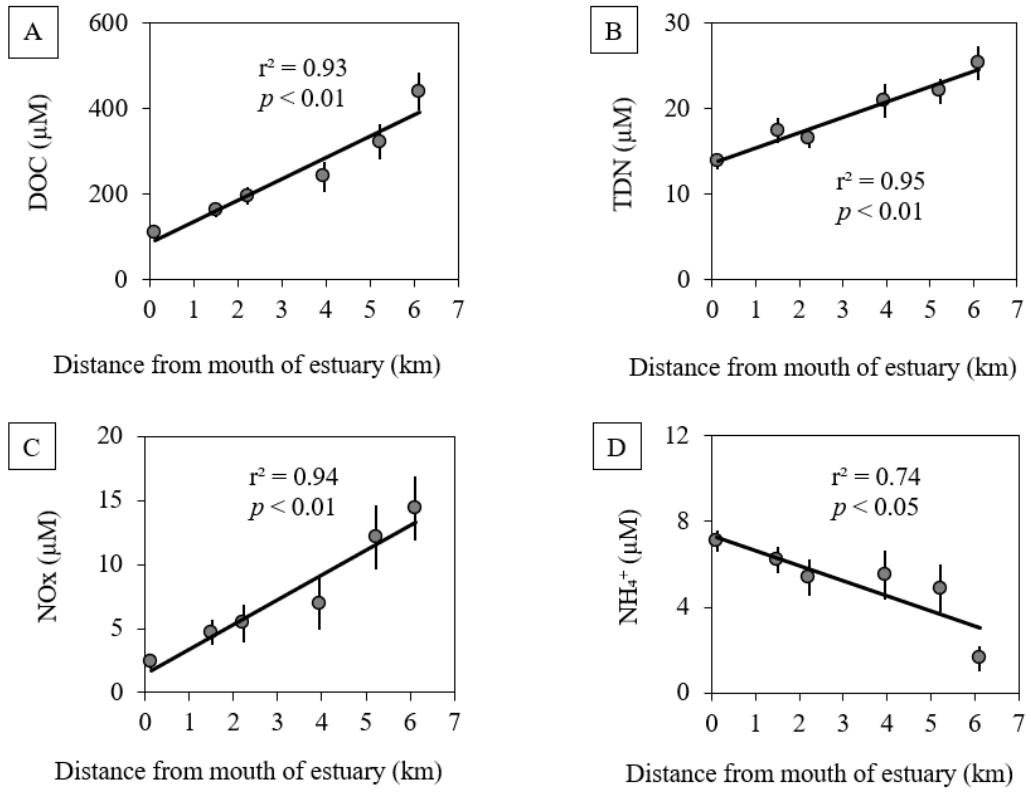

Figure 3. (A) Near-surface dissolved organic carbon (DOC), (B) total dissolved nitrogen (TDN), (C) nitrate + nitrite (NO_X) patterns of linear reduction, and (D) ammonium (NH_4^+) pattern of linear increase from the upper estuary to the lower estuary in Coffs Creek, Australia. Data points are annuals with error bars representing intra-annual variance (calculated as SE).

Annual upstream average NH_4^+ concentrations of 1.4 µM exceeded ANZECC water quality guidelines for lowland streams (ANZECC, 2000), with an isolated 5-fold spike over guidelines in May 2018 with no preceding rainfall (BOM, 2021a). Annual downstream NH_4^+ concentrations were, on average, 7-fold over ANZECC water quality guidelines for estuaries of 1.1 µM (ANZECC, 2000), with concentrations consistently breaching ANZECC guidelines every month between 4 and 9-fold. NH_4^+ concentration spikes had no correlation with rainfall.

The highest NO_X concentrations of 14.4 ± 4.7 µM were found in the upper estuary with concentrations peaking in high rainfall periods. Annual upstream NO_X concentrations were, on average, 5-fold over ANZECC water quality guidelines for lowland streams of 2.9 µM (ANZECC, 2000). Upstream NO_X concentrations peaked at 14-fold over ANZECC water quality guidelines in July and in March respectively, after accumulated runoff > 20 mm m^{-2} day^{-1} in both months (BOM, 2021a). However, upstream NO_X concentrations were generally lower than found in nearby Double Crossing Creek upper estuary (48.5 ± 26.7 µM), likely due to a combination of a smaller percentage of horticulture land use in the Coffs Creek catchment and the dry conditions from November to

February resulting in low soil moisture (22%) limiting DIN transport into the estuary (White et al., 2018).

Annual downstream NO_X concentrations were, on average, 2-fold over ANZECC water quality guidelines for estuaries of 1.1 µM (ANZECC, 2000). Downstream NO_X concentrations peaked at 5-fold over ANZECC water quality guidelines in July and March, correlating with the accumulated runoff of > 20 mm m^{-2} day^{-1}. Average NO_X concentrations were 3-fold higher in July 2017 (23.4 ± 6.3 µM), than the annual mean at all sites (8.0 ± 0.6 µM), coinciding with a > 250 mm in 20 days flood event. There was 304 mm total rainfall and soil moisture reached a maximum of 87% in the month prior to the July sampling (BOM, 2021a, 2021b). Subsequent rain events in March 2018 (24.6 ± 6.3 µM) and June 2018 (19.1 ± 4 µM) also revealed elevated NO_X concentrations 3 and 2-fold higher than the annual mean, respectively. High soil moisture (~ 80%) immediately preceding the elevated concentrations of NO_X was also recorded in March.

Incoming nutrient fluxes deposited NO_X loads of ~ 109 ± 82 kg km^{-2} $year^{-1}$ into the upper estuary. High NO_X attenuation (average of 81%) occurred from upstream to downstream, reducing downstream loads exported to the Solitary Islands Marine Park to ~ 18 ± 12 kg km^{-2} $year^{-1}$. In contrast, incoming nutrient fluxes deposited small NH_4^+ loads of ~ 3 ± 1 kg km^{-2} $year^{-1}$ into the upper estuary. High NH_4^+ accretion occurred from upstream to downstream, increasing downstream loads exported to the Solitary Islands Marine Park to ~ 22 ± 11 kg km^{-2} $year^{-1}$.

Estuaries are generally considered dynamic N transformation hotspots due to hydrodynamic fluctuations driving nitrogen cycling through nitrification and denitrification (Wong et al., 2018). In dry conditions, water flow decreases, and instream N cycling increases due to the increased residence time of the water. Catchment N exports to waterways are generally driven by hydrology and land use (White et al., 2018; Wong et al., 2018). NO_X is often the main form of nitrogen in urban and suburban catchments (Harris, 2001; Kaushal et al., 2011) such as Coffs Creek estuary. The higher nutrient loading in the upper part of the estuary and less efficient tidal flushing likely increased residence time in dry periods and drove eutrophic conditions, contributing to the low DO found in the upper catchment.

NOx concentrations of zero were observed through the mangrove-dense areas of the estuary in months with < 5mm rainfall, revealing sinks of NO_X in dry conditions. Low DO levels (< 25%), coupled with low NO_X in the dry period between August and October, were observed in the mangrove-dense areas, potentially increasing the denitrification rates, and driving sinks of N (Tait et al., 2017). DOC was generally available and likely did not inhibit denitrification processes, as implied from the higher concentrations in the upper estuary compared to the lower estuary concentrations. The

reductions of TDN and NO_X down the estuary may be attributed to mangrove nutrient uptake or instream N cycling.

In this study, the most extensive mangrove-dominated section of Coffs Creek estuary revealed potential uptake of 17.8 μmol m^{-2} day^{-1} NO_X during dry conditions and produced 3.6 μmol m^{-2} day^{-1} NH_4^+. This equates to a net removal of 14.2 μmol m^{-2} day^{-1} of DIN overall. These results suggest that mangrove ecosystems reduce net N loads by uptake of N from the creek waters. Estuaries with high mangrove density can uptake NO_X as high rates of porewater deliver NO_X to mangrove roots (Maher et al., 2016). Porewater exchange occurs within complex underground structures, with the high amount of organic matter sediment and the nitrate inflows stimulating complete denitrification and nitrate uptake by roots (Tait et al., 2017; Maher et al., 2016). Complete biological denitrification within mangrove sediments occurs as denitrifying microbes reduce NO_X to N_2 (Erler et al., 2015; Maher et al., 2016;). This NO_X conversion process occurs in low oxygen settings which are optimal for denitrification (Venkiteswaran et al., 2014). The lower DO saturations upstream also suggest that denitrification is likely the main loss pathway of NO_X in the upper estuary in dry conditions (Welti et al., 2017).

Earlier seasonal and tidal-scale investigations conducted in Coffs Creek found that the mangrove-dominated section of the estuary was a sink of NO_X during dry conditions (Reading et al., 2017; Reading et al., 2020). Here, the same mangrove-dominated section of the estuary also revealed NO_X reduction in dry conditions with high attenuation (~ 91%) during low flow times. In coastal areas, estuarine processes have been shown to attenuate 30% to 65% of DIN (Nixon et al., 1996). Our observations found Coffs Creek estuary DIN attenuation rates are above the higher estimates of Nixon et al. (1996). These results suggest that mangrove ecosystems significantly reduce net N loads to the ocean. As mangroves may play a critical role in cycling N, conserving fringe mangroves in estuarine environments is beneficial to estuarine water quality by buffering aquatic nitrogen exports the ocean (Jickells et al., 2017; Wadnerkar et al., 2019).

3.2 Flood observations

3.2.1 Hydrological conditions over a flood scale

A 94.9 mm rain event was captured from the 3rd – 13th March 2018 which increased soil moisture from 57% to 84% on the highest day of rainfall (Table 3). Detailed time-series observations at the upstream and downstream episodic sites revealed changes in physicochemical parameters, DOC, and nitrogen species (Figure 4). Observations commenced three days prior to the rain to build baseline conditions and are described as ‘Pre-rain’. The highest rainfall was observed on the 7th of March and described as ‘Rain’, with 70% of the event's total rainfall (64.6 mm) on this day. The maximum discharge of 3.09 m^3 s^{-1} occurred twenty-four hours after the initial rain event on post-rain ‘Day 1’ (8th

March) with 1 mm of rain on this day. Lighter falls (14.2 mm and 8.2 mm) were observed, on Days 2 and 3, as the rain event dissipated.

Water temperature during the flood was 22.3 ± 0.1°C and 23.8 ± 1.3°C at the upstream and downstream stations, respectively. The upstream temperature remained consistent while the downstream pre-rain temperature was 25.1 ± 0.1°C, falling to 23.6 ± 0.3°C on the day of highest rain, and slowly rising back to 25.1 ± 0.6°C by Day 6 (post-rain) as runoff reduced. Throughout the flood, upstream salinity values remained close to zero (0.1 ± 0.03), with no tidal influence. Downstream salinity varied from 2.1 to 35.4 and was 26.6 at the first low tide pre-rain, dropping following the peak of the flood, 10 hours after rain and during the low tide, to near-freshwater values.

Upstream DO was consistently undersaturated (70 ± 2.7%) with the lowest saturation of 31% observed pre-rain. Downstream DO fluctuated with the tides with an initial reduction to 75 ± 2.6% during rain from pre-rain baseline saturation of 94 ± 0.1%. Mean daily DO saturations increased as rain intensity increased at the peak of the flood to 79.6 ± 3.15% (high tide 97.1% DO, low tide 66.7% DO). There was a general trend of DO increase after the peak rainfall, reaching 86 ± 2.4% by Day 6.

Table 3. Daily rainfall, runoff, and soil moisture values for each of the eight periods before, during, and after the episodic rain event in Coffs Creek estuary, NSW, Australia (BOM, 2021a, 2021b).

	Rainfall (mm)	**Runoff (mm m^{-2} day^{-1})**	**Root zone soil moisture (%)**
Pre-rain	5.3	0.08	57
Rain	64.6	5.87	84
Day 1	1	4.84	81
Day 2	14.2	3.98	81
Day 3	8.2	3.08	82
Day 4	1.6	2.13	80
Day 5	0	1.47	78
Day 6	0	1.02	76
Total	94.9	22.47	n /a

3.2.2 Nitrogen species and dissolved organic carbon over a flood scale

All upstream nutrient concentrations were higher during and immediately after rainfall and as runoff increased, carrying soil stored nutrients into the creek. Upstream nutrient concentrations were consistently high with little variability, unaffected by tidal influence. Downstream nutrient concentrations were highly variable over tidal time scales. At high tide, downstream values reduced as a result of dilution caused by seawater penetration into the estuary. During low tide, the downstream concentrations increased due to freshwater runoff moving nutrients towards the SIMP.

Dissolved organic nitrogen (DON) was an important N form in surface waters at the upstream (~ 40% of TDN) and downstream stations (~ 46% of TDN). NO_X was ~ 60% of TDN and the main form of DIN upstream (~ 98%), and downstream (~ 77%). Upstream DOC was readily available and rose with rain to 468.2 ± 63 µM, peaking on Day 1 at 583.7 µM. Downstream DOC fluctuated with the tides after an initial rise with rain to 89.8 ± 13.8 µM, peaking on Day 1 at 120.3 µM.

DON, NO_X and NH_4^+ values rose during the high flow periods and slowly fell over the following 6 days with downstream periodic values rising and falling with the tides (Figure 4). Upstream NOx concentration was 44.7 ± 5.3 µM reaching 94.2 µM at the peak of discharge. Pre-rain downstream NO_X concentrations were 0.8 ± 0.1 µM, increasing to 21.6 ± 4.3 µM during rain. Low tide downstream NO_X concentrations reached 46.2 µM at the peak of the flood. By Day 6 (post-rain), downstream NO_X concentrations (2.7 ± 0.9 µM) were still above pre-rain concentrations.

Flood upstream NO_X concentrations were, on average, 16-fold over ANZECC water quality guidelines of 2.9 µM for lowland streams and peaked at 34-fold over ANZECC. Flood downstream NO_X concentrations were, on average, 9-fold over ANZECC water quality guidelines of 1.1 µM for estuaries and peaked at 43-fold over ANZECC.

Flood upstream NH_4^+ concentrations were, on average, within ANZECC water quality guidelines of 1.4 µM for lowland streams and peaked at 2-fold over ANZECC. Flood downstream NH_4^+ concentrations were, on average, 2.5-fold over ANZECC water quality guidelines of 1.1 µM for estuaries and peaked at 13-fold over ANZECC.

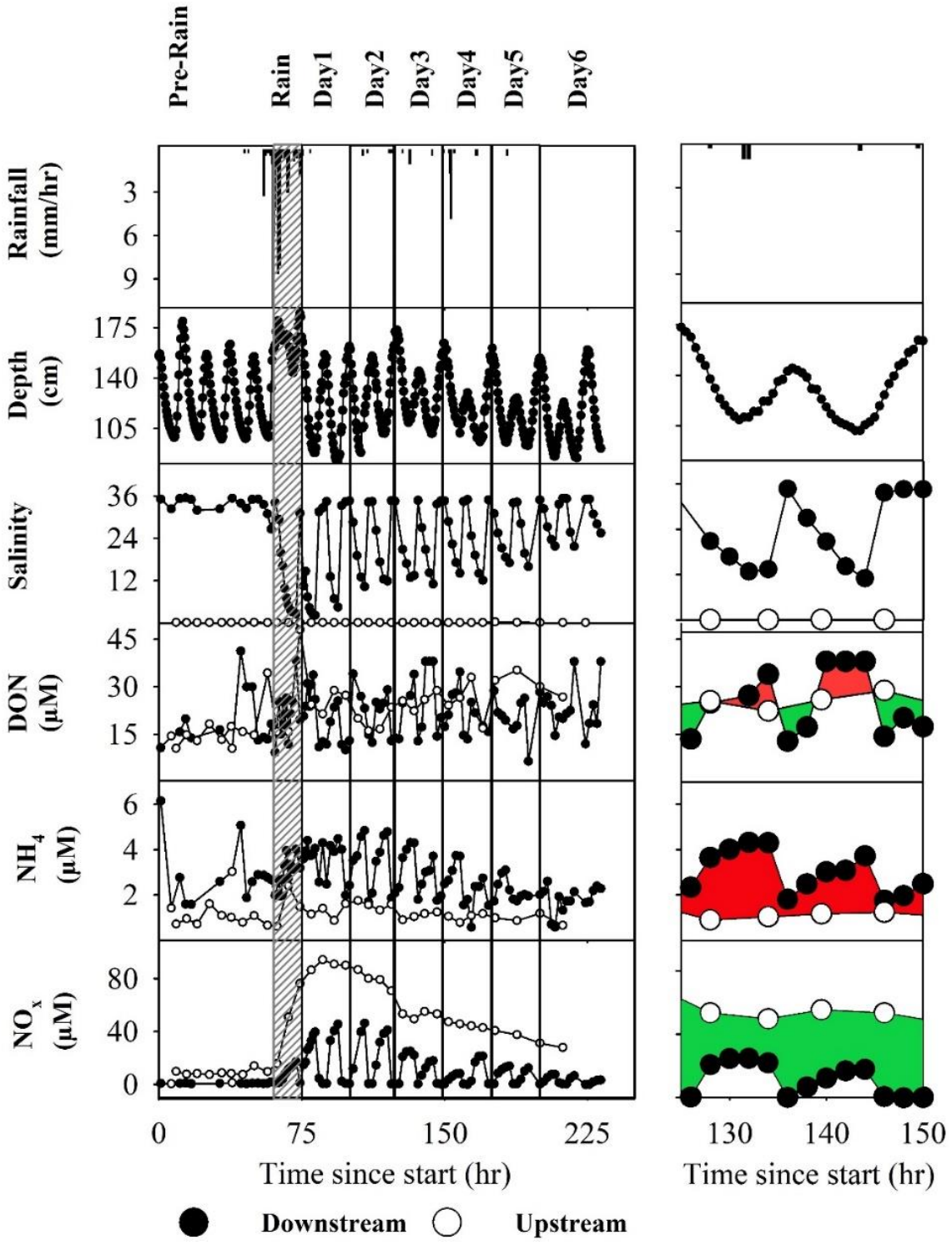

Figure 4. Time-series observations of hourly rainfall and water chemistry parameters collected over two hundred and thirty-two hours (3rd to 13th March 2018). The left stack shows all the samples, while the right stack zooms in two tidal cycles. The green shading indicates a removal of nitrogen between the upstream and downstream stations, while the red shading indicates an addition of nitrogen. The scale of the nitrate removal is much larger than the DON and ammonium addition (Wadnerkar et al., 2019).

The major increase in NO_X levels found in the upper estuary after rainfall likely resulted from freshwater nutrient inputs to the creek, originating from fertilisers used in intensive agriculture (White et al., 2018) and urban land use (Wong et al., 2018). Large amounts of NO_X can leach into coastal river systems and subsequent estuaries due to farming practices in upper catchment areas having low efficiency of fertiliser use (White et al., 2018; Zhang et al., 2019). NO_X can be stored in the soil during dry conditions and flushed into waterways during heavy rainfall (Van Meter et al., 2016; White et al., 2021a).

Hydrology is a major driver of NO_X from upper estuary areas to lower estuary areas (White et al., 2020). Our results and other studies show that NO_X exports from land to the ocean are greatly influenced by rainfall (White et al., 2018; Wong et al., 2018; Wadnerkar et al., 2019; White et al., 2021a). Smaller creek systems in this region have been shown to export more NO_X from upstream to downstream during high rainfall and increased flow periods (Wadnerkar et al., 2019; White et al., 2021a). The decrease in salinity during and post-rain suggests that nutrient concentrations (particularly NO_X) in Coffs Creek estuary are heavily influenced by creek discharge flushing events (Figure 4).

The flushing time of Coffs Creek estuary in pre-rain conditions was ~ 25 days, while in the flood event, flushing time was less than 1 day (Wadnerkar et al., 2019). During and directly after the heavy rainfall, increased freshwater flow in the estuary flushed upstream NO_X loads directly towards the ocean. NO_X concentrations at the downstream station were lower than at the upstream station (Figure 5) providing initial evidence of nitrogen cycling or losses/uptake of nitrogen within the estuary. However, mean NO_X loads at the downstream station during rain and post-rain conditions were > 5-fold higher than pre-rain, suggesting that natural stream nutrient attenuation processes were overwhelmed during heavy NO_X loading.

Average NH_4^+ concentrations (2.8 µM) at the downstream station were 2.5-fold higher than the upstream station. While only a fraction of DIN observed in Coffs Creek estuary was NH_4^+ (upstream ~ 2 %, downstream ~ 23 %), these results suggest some conversion of upstream NO_X into NH_4^+ along the estuary likely due to tidally driven pore water exchange within the anoxic estuarine mangrove sediments (Wadnerkar et al., 2019) and potential NH_4^+ inputs from urban sources along the creek.

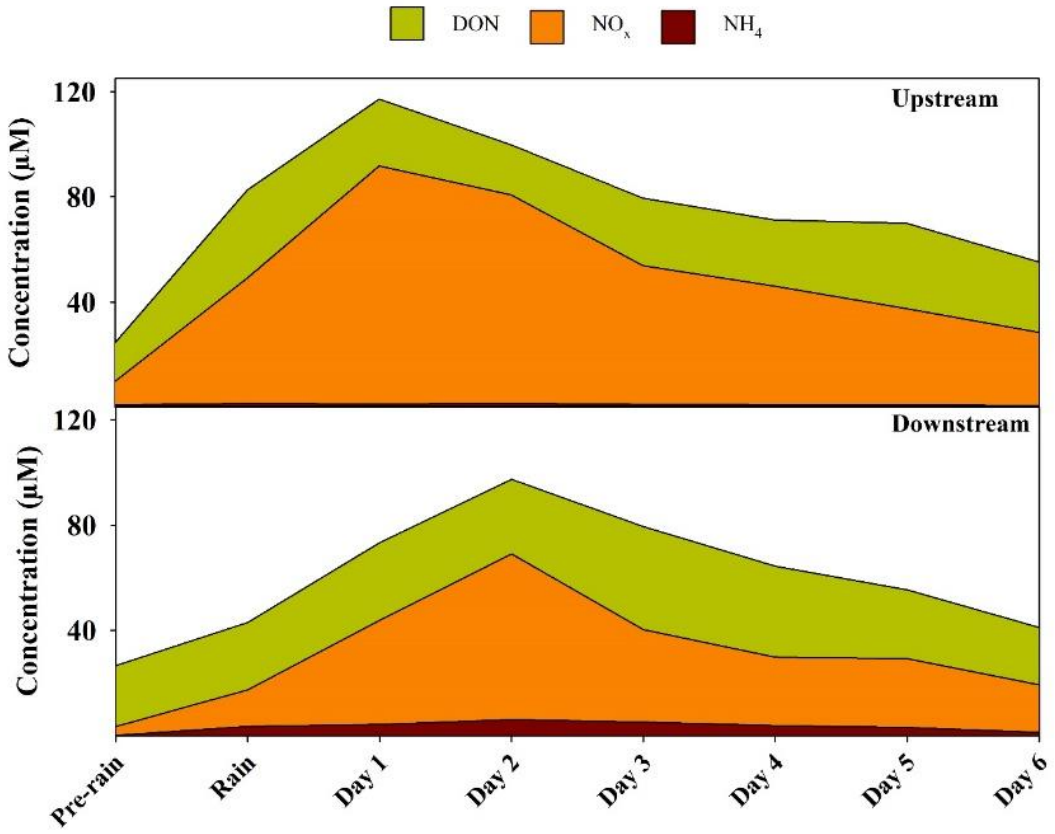

Figure 5. Nitrogen species (NH_4^+, NO_x, and DON) pre-, during, and post-rain at the upstream and downstream time series stations (Wadnerkar et al., 2019).

Nutrient concentrations were plotted against salinity (Figure 6) to show the effective freshwater N concentrations draining to the ocean. NO_X showed an inverse relationship with salinity in the various time stages, while the correlations of DON and NH_4^+ were not as clear. Extrapolating the relationship back to the zero-salinity intercept revealed a clear attenuation of NO_X loads during transport along the estuary. The maximum TDN attenuation was observed during the larger, initial rainfall period of the flood (48% attenuation).

High NO_X attenuation (71%) occurred during the initial day of the rain event (Figure 7) when downstream loads, exported to the SIMP, were 31 µmol m^{-2} day^{-1} (Figure 8). As NO_X loads increased, instream attenuation was overwhelmed. The increased sediment and water transport coincided with a significant reduction in creek attenuation capacity. Downstream NO_X loads peaked 48 hrs later at 649 µmol m^{-2} day^{-1} with attenuation reduced to 20% from upstream inputs of 817 µmol m^{-2} day^{-1}. While mangrove uptake and in stream attenuation capacity were major contributors of N removal in dry to moderately wet conditions, the increased discharge during flood conditions overwhelmed natural ecosystem processes and elevated N loads.

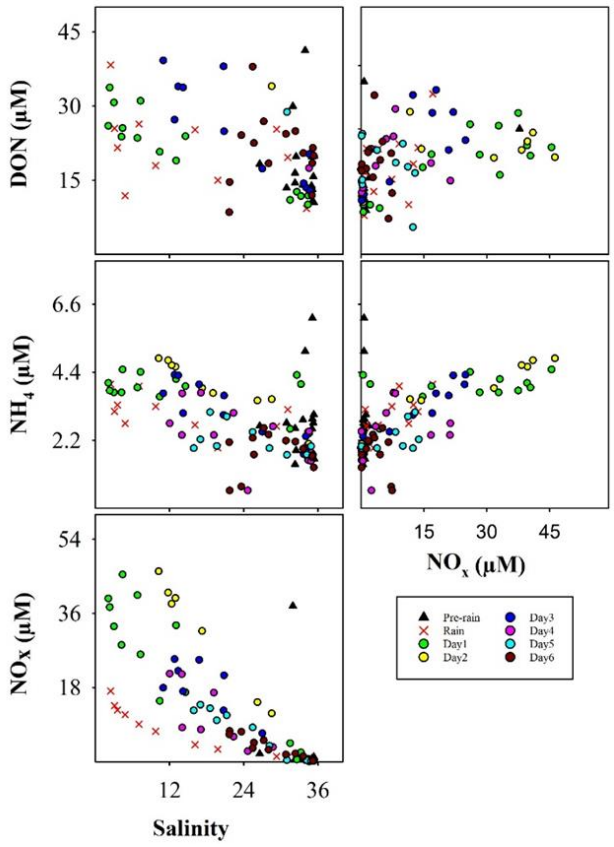

Figure 6. Scatter plots of salinity versus NOx concentration and NOx concentration versus NH_4^+ and DON (pre-, during, and post-rain, as well as during the individual precipitation events (Wadnerkar et al., 2019).

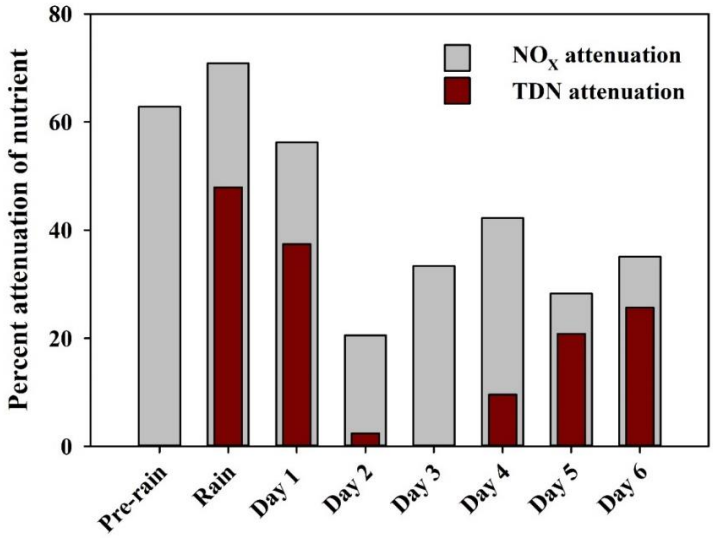

Figure 7. Bar chart showing the percent retention of the Coffs Creek estuary (NO_x and TDN) (Wadnerkar et al., 2019).

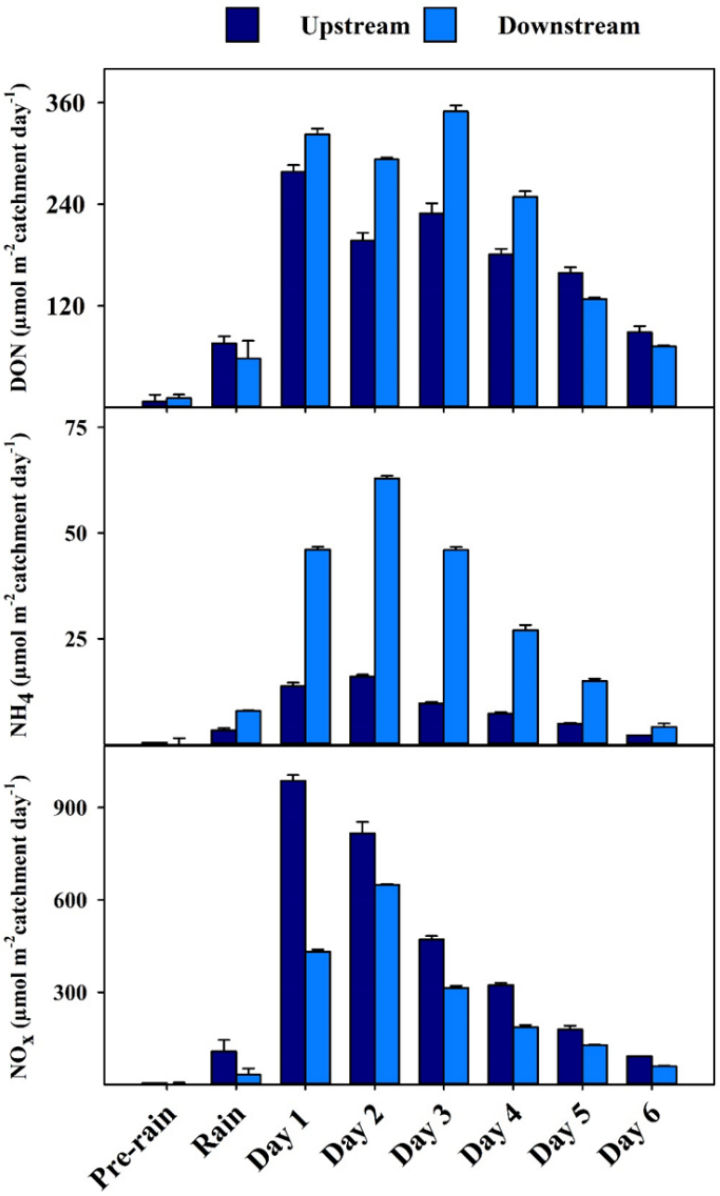

Figure 8. Nitrogen loads of surface water from upstream and downstream time-series stations. Note the different scales for NO_X, NH_4^+, and DON (Wadnerkar et al., 2019).

3.3 Annual and flood comparisons

The captured flood event created a 'hot moment', driving elevated NO_X concentrations through the estuary. The peak upstream flood March NO_X observation (94.2 µM) was ~ 2-fold higher than the upstream annual March NO_X observation (41.3 µM) (Figure 9). The peak downstream low tide flood March NO_X observation (46.2 µM) was ~ 8-fold higher than the downstream low tide annual March NO_X observation (5.9 µM).

Imported NO_X loads to the upper estuary temporarily increased from 21.4 µmol m^{-2} day^{-1} to 42.1 µmol m^{-2} day^{-1} (Figure 10). Exports of NO_X loads to the SIMP temporarily increased from 3.5 µmol m^{-2} day^{-1} to 5.3 µmol m^{-2} day^{-1}. Incorporating the flood observation into the annual lower estuary estimates will increase NO_X loading 5-fold from ~ 18 ± 12 kg km^{-2} $year^{-1}$ to ~ 99 ± 92 kg km^{-2} $year^{-1}$, significantly increasing exports to the SIMP. Capturing the flood revealed insights beyond what can be obtained from seasonal or monthly sampling. For example, the monthly sample taken after the flood in March missed the large NO_X spike entirely. Whilst there is elevated nitrogen, in particular NO_X, in the spatial observation in March 2018, monthly spatial observations neglected the peak NO_X imports during high rainfall.

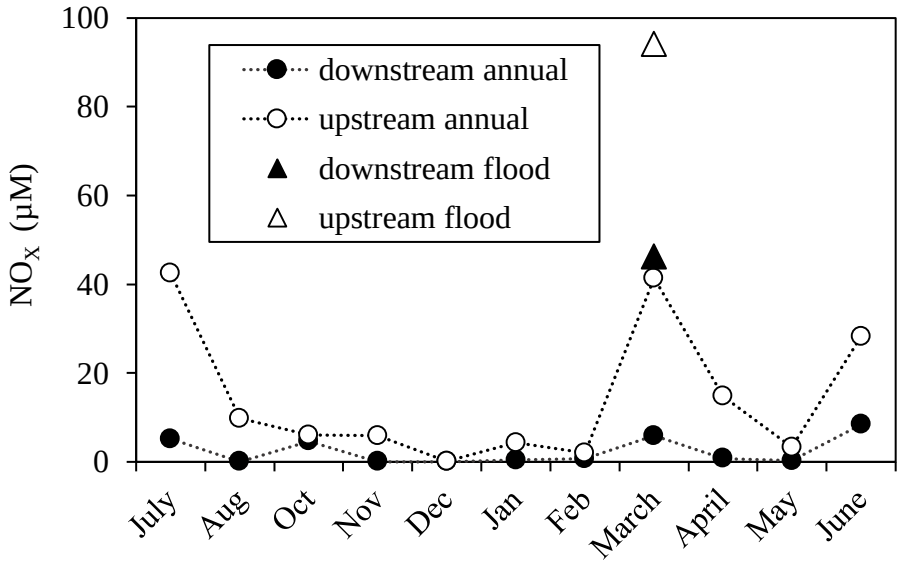

Figure 9. NO_X concentrations in Coffs Creek estuary over annual scales and at peak flood conditions. White circles represent monthly surveys upstream and black circles represent monthly surveys downstream. The white triangle represents peak flood observation upstream, and the black triangle represents peak flood observation downstream. Only low tide time-series observations were utilised to reduce tidal bias. In March, the monthly NO_X observation was taken six days after the rain-event NO_X observation. The increase in NO_X captured during the rain event is the difference between the spatial March observation and the peak flood observation.

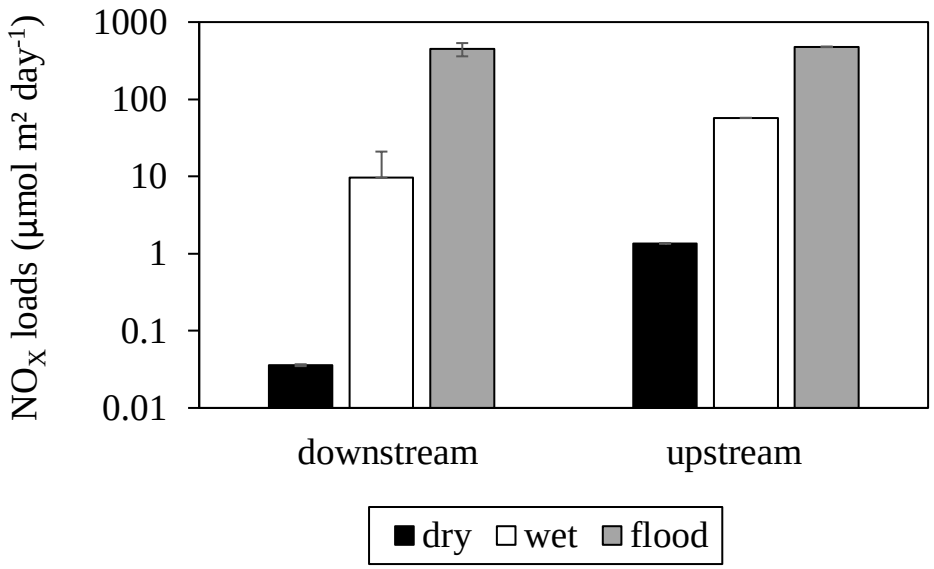

Figure 10. Comparison of NO_X loads upstream and downstream of Coffs Creek estuary in dry, wet, and flood conditions. Error bars are standard error.

Monthly observations over an annual time scale found no statistical relationship between runoff and NO_X concentrations (Figure 11A) or root zone soil moisture and NO_X concentrations (Figure 11B) upstream or downstream. However, a strong significant relationship was revealed between runoff and NO_X upstream ($r^2 = 0.96$, $p < 0.01$) and downstream ($r^2 = 0.96$, $p < 0.01$) during intensive flood sampling (Figure 11C). A strong and significant exponential relationship was revealed between root zone soil moisture and NO_X concentrations both upstream ($r^2 = 0.88$, $p < 0.05$) and downstream ($r^2 = 0.93$, $p < 0.01$) (Figure 11D). The sharp rise in NO_X concentrations occurred after root zone soil moisture saturation of 70%.

Changes in soil moisture can affect N cycling through changes in microbe activity and oxygen availability for microbe colonies (Hajati et al., 2020). Water content in the soil controls the transport of oxygen into the soil and the transport of NO_X out of the soil (Pilegaard, 2013) as NO_X is highly soluble in water (Puckett, 1994). In periods of low rainfall, dry and aerated soils encourage nitrification within the N cycle, transforming NH_4^+ to NO_X, increasing the NO_X storage in the soil (Davidson et al., 2000). NO_X can be stored in catchment soils and flushed into waterways via runoff during rain events when soil moisture increases (Van Meter et al., 2016). Our result indicating that there may be a tipping point of nutrient release from ~ 70% saturation point supports the results of other studies. A study performed in a close-by catchment found that the threshold limit of upstream soil storage was at 40% soil moisture, where NO_X was transported to the creek with runoff and increased as soil moisture increased (White et al., 2020).

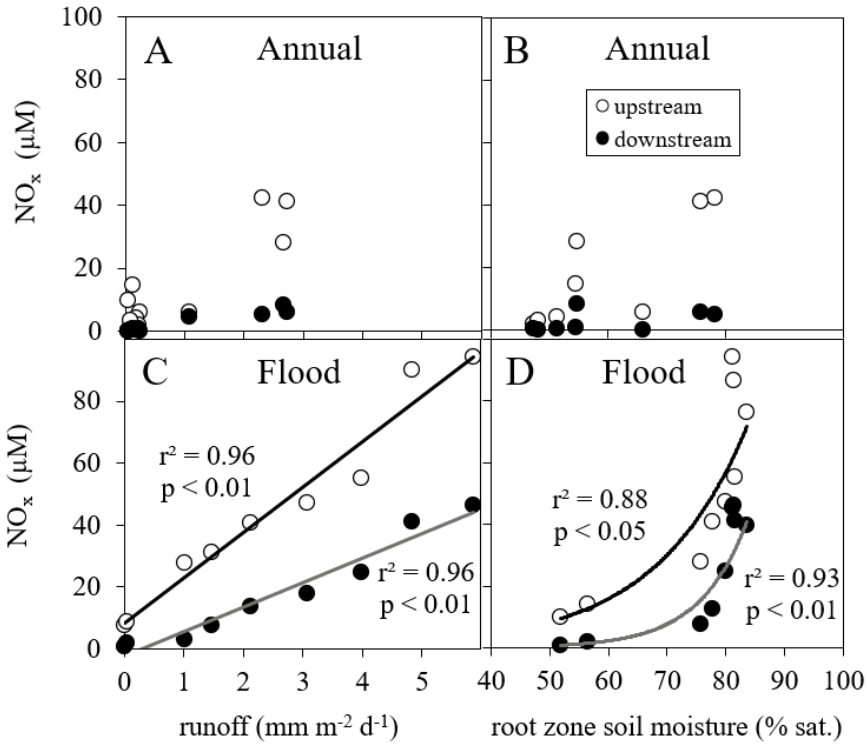

Figure 11. Monthly (A) NO_X concentration versus runoff, (B) NO_X concentration versus soil moisture and flood (C) NO_X concentration versus runoff, (D) NO_X concentration versus soil moisture. Linear trendlines indicate a steady increase in runoff over the flood event while the exponential trendlines indicate a sharp and rapid increase in NO_X concentrations during the flood.

4. Conclusion

Estuarine N concentrations and loads were quantified in Coffs Creek estuary across a salinity gradient, with monthly observations over an entire year coupled with detailed high-resolution observations during a minor flood event. NO_X was the main form of dissolved inorganic nitrogen (DIN) at the furthermost upstream site of the estuary (~ 90%), while NH_4^+ was the main form of DIN at the most downstream site (~ 75%). Annual upstream NO_X concentrations were, on average, 5-fold over ANZECC water quality guidelines, peaking at 14-fold over ANZECC water quality guidelines in July and March after accumulated runoff > 20 mm m^{-2} day^{-1}. Annual downstream NH_4^+ concentrations were, on average, 7-fold over ANZECC water quality guidelines, with concentrations consistently breaching guidelines every month between 4 and 9-fold.

Strong wet-dry variability was observed with a change from low N loads reaching the SIMP during dry conditions to high N loads during episodic rainfall. Overall, loads of NO_X were high and NH_4^+ loads were low coming into the estuary from the upper catchment over an annual scale when using monthly observations. Incoming nutrient fluxes deposited NO_X loads of ~ 109 ± 82 kg km^{-2} $year^{-1}$ into

the upper estuary. High NO_X attenuation (average of 81%) occurred from upstream to downstream, reducing downstream loads exported to the Solitary Islands Marine Park to ~ 18 ± 12 kg km^{-2} $year^{-1}$. In contrast, incoming nutrient fluxes deposited small NH_4^+ loads of ~ 3 ± 1 kg km^{-2} $year^{-1}$ into the upper estuary. High NH_4^+ accretion occurred from upstream to downstream, increasing downstream loads exported to the Solitary Islands Marine Park to ~ 22 ± 11 kg km^{-2} $year^{-1}$.

NO_X attenuation was high (71%) during the initial day of the flood. As NO_X loads increased, instream attenuation was overwhelmed. The increased sediment and water transport coincided with a significant reduction in creek attenuation capacity (20%). While mangrove uptake and in-stream attenuation capacity were major contributors of N removal in dry to moderately wet conditions, the increased discharge during flood conditions interrupted natural ecosystem processes.

Our results demonstrated that the mangrove-dominated estuary was an effective removal pathway of NO_X in the dry and moderately wet months through attenuation. Seasonal variation was prominent in the attenuation of N in the mangrove dominated sections of the creek, while flood events potentially reduce natural creek NO_X attenuation capacity and elevate N loads. Flood events greatly increase catchment NO_X imports into the Coffs Creek estuary, overwhelming in-stream N removal processes, and subsequently greatly increase NO_X exports to the SIMP.

5. Recommendations

- **Capture rainfall events in temporary storage basins on farm.** Rapid estuarine flushing prevents the natural removal of nitrogen by mangroves within the estuary. The construction of dams and reservoirs on horticulture properties would slow down catchment flushing, allowing nitrogen-enriched water to be released at a later time when mangroves would be able to remove most of the nitrogen.

- **Reducing N inputs through more efficient application of fertilisers**. A reduction in the amount and concentration of fertiliser applied in the upper catchment will reduce N loading and increase the N attenuation capacity of the Coffs Creek estuary (White et al., 2020). This intervention may reduce excess nutrient waste moving off-site in drainage. This runoff can be both detrimental to the farmer, through the economic loss of excess fertiliser and to the environment, through downstream impacts of runoff entering soil and waterways.

- **Deploy constructed N filters.** Anthropogenic N removal mechanisms may be considered for regulation and filtration of upper catchment farm runoff before it enters the estuary waters.

Complementary solutions such as horizontal subsurface constructed wetlands (Grasselly et al., 2005), riparian zones (Hill, 2019) and bioreactors (Kjaersgaard et al., 2014) are options to reduce nitrogen pollution. The solution can be coupled to water storage basins that allow for slower transport of nitrogen-enriched waters.

- **Protect mangroves.** Mangroves are an important part of in-stream attenuation processes, playing a critical role in reducing N concentrations and cycling N. Conserving existing fringe mangroves and increasing the density of mangroves habitats in estuarine environments through the construction of mangrove nurseries is beneficial to estuarine water quality by buffering aquatic nitrogen exports the ocean.

6. References

Addy, K., Gold, A., Nowicki, B., McKenna, J., Stolt, M., & Groffman, P. (2005). Denitrification capacity in a subterranean estuary below a Rhode Island fringing salt marsh. *Estuaries*, *28*(6), 896–908.

Adyel, T. M., Oldham, C. E., & Hipsey, M. R. (2016). Stormwater nutrient attenuation in a constructed wetland with alternating surface and subsurface flow pathways: Event to annual dynamics. *Water Research*, *107*, 66–82.

Alongi, D. M. (2002). Present state and future of the world's mangrove forests. *Environmental Conservation*, *29*(3), 331–349.

Andrews, L. F., Wadnerkar, P. D., White, S. A., Chen, X., Correa, R. E., Jeffrey, L. C., & Santos, I. R. (2021). Hydrological, geochemical and land use drivers of greenhouse gas dynamics in eleven sub-tropical streams. *Aquatic Sciences*, *83*(2), 1–19.

Australian and New Zealand Environment and Conservation Council [ANZECC]. (2000). *Australian and New Zealand Guidelines for Fresh and Marine Water Quality*. Canberra, Australia: Australian and New Zealand Environment and Conservation Council, Agriculture and Resource Management Council of Australia and New Zealand.

Australian Government Bureau of Meteorology [BOM]. (2021a). *Australian Landscape Water Balance (AWRA-L v6)*.

Australian Government Bureau of Meteorology [BOM]. (2021b). *Climate Data Online*.

BMT WBM. (2011). *Coffs Harbour Coastal Processes and Hazards Definition Study Final Report*. Coffs Harbour City Council.

Borges, A. V., Darchambeau, F., Lambert, T., Bouillon, S., Morana, C., Brouyère, S., Hakoun, V., Jurado, A., Tseng, H.-C., & Descy, J.-P. (2018). Effects of agricultural land use on fluvial carbon dioxide, methane and nitrous oxide concentrations in a large European river, the Meuse (Belgium). *Science of the Total Environment*, *610*, 342–355.

Butterbach-Bahl, K., Baggs, E. M., Dannenmann, M., Kiese, R., & Zechmeister-Boltenstern, S. (2013). Nitrous oxide emissions from soils: How well do we understand the processes and their controls? *Philosophical Transactions of the Royal Society B: Biological Sciences*, *368*(1621), 20130122.

Coffs Harbour City Council. (2020). *Coffs Creek Coastal Zone Management Plan*.

Conrad, S. R., Sanders, C. J., Santos, I. R., & White, S. A. (2018). Investigating water quality in Coffs coastal estuaries and the relationship to adjacent land use. Part 1: Sediments. National Marine Science Centre, Southern Cross University, Coffs Harbour. *NSW*, *42*.

Conrad, S. R., Santos, I. R., Brown, D. R., Sanders, L. M., van Santen, M. L., & Sanders, C. J. (2017). Mangrove sediments reveal records of development during the previous century (Coffs Creek estuary, Australia). *Marine Pollution Bulletin*, *122*(1–2), 441–445.

Conrad, S. R., Santos, I. R., White, S. A., Hessey, S., & Sanders, C. J. (2020). Elevated dissolved heavy metal discharge following rainfall downstream of intensive horticulture. *Applied Geochemistry*, *113*, 104490.

Davidson, E. A., Keller, M., Erickson, H. E., Verchot, L. V., & Veldkamp, E. (2000). Testing a conceptual model of soil emissions of nitrous and nitric oxides: Using two functions based on soil nitrogen availability and soil water content, the hole-in-the-pipe model characterizes a large fraction of the observed variation of nitric oxide and nitrous oxide emissions from soils. *Bioscience*, *50*(8), 667–680.

Emerson, S., Jahnke, R., & Heggie, D. (1984). Sediment-water exchange in shallow water estuarine sediments. *Journal of Marine Research*, *42*(3), 709–730.

Erler, D. V., Duncan, T. M., Murray, R., Maher, D. T., Santos, I. R., Gatland, J. R., Mangion, P., & Eyre, B. D. (2015). Applying cavity ring-down spectroscopy for the measurement of dissolved nitrous oxide concentrations and bulk nitrogen isotopic composition in aquatic systems: Correcting for interferences and field application. *Limnology and Oceanography: Methods*, *13*(8), 391–401.

Eyre, B. (1997). Water quality changes in an episodically flushed sub-tropical Australian estuary: A 50 year perspective. *Marine Chemistry*, *59*(1–2), 177–187.

Eyre, B. D. (2000). Regional evaluation of nutrient transformation and phytoplankton growth in nine river-dominated sub-tropical east Australian estuaries. *Marine Ecology Progress Series*, *205*, 61–83.

Grasselly, D., Merlin, G., Sédilot, C., Vanel, F., Dufour, G., & Rosso, L. (2004). Denitrification of soilless tomato crops run-off water by horizontal subsurface constructed wetlands. *International Conference on Sustainable Greenhouse Systems-Greensys2004 691*, 329–332.

Hajati, M.-C., White, S., Moosdorf, N., & Santos, I. R. (2020). Modeling catchment-scale nitrogen losses across a land-use gradient in the subtropics. *Frontiers in Earth Science*, 347.

Harris, G. P. (2001). Biogeochemistry of nitrogen and phosphorus in Australian catchments, rivers and estuaries: Effects of land use and flow regulation and comparisons with global patterns. *Marine and Freshwater Research*, *52*(1), 139–149.

Herbeck, L. S., Unger, D., Krumme, U., Liu, S. M., & Jennerjahn, T. C. (2011). Typhoon-induced precipitation impact on nutrient and suspended matter dynamics of a tropical estuary affected by human activities in Hainan, China. *Estuarine, Coastal and Shelf Science*, *93*(4), 375–388.

Hill, A. R. (2019). Groundwater nitrate removal in riparian buffer zones: A review of research progress in the past 20 years. *Biogeochemistry*, *143*(3), 347–369.

Jickells, T. D., Buitenhuis, E., Altieri, K., Baker, A. R., Capone, D., Duce, R. A., Dentener, F., Fennel, K., Kanakidou, M., & LaRoche, J. (2017). A reevaluation of the magnitude and impacts of anthropogenic atmospheric nitrogen inputs on the ocean. *Global Biogeochemical Cycles*, *31*(2), 289–305.

Jordan, S. J., Stoffer, J., & Nestlerode, J. A. (2011). Wetlands as sinks for reactive nitrogen at continental and global scales: A meta-analysis. *Ecosystems*, *14*(1), 144–155.

Kaushal, S. S., Groffman, P. M., Band, L. E., Elliott, E. M., Shields, C. A., & Kendall, C. (2011). Tracking nonpoint source nitrogen pollution in human-impacted watersheds. *Environmental Science & Technology*, *45*(19), 8225–8232.

Kjaersgaard, J., Moorman, T., David, M., Schipper, L., & Feyereisen, G. (2014). Know Your Community: Managing Denitrification in Agronomic Systems. *Crops, Soils, Agronomy News*, *59*(5), 28–29.

Maher, D. T., Sippo, J. Z., Tait, D. R., Holloway, C., & Santos, I. R. (2016). Pristine mangrove creek waters are a sink of nitrous oxide. *Scientific Reports*, *6*(1), 1–8.

Masselink, G., & Gehrels, R. (2015). Introduction to coastal environments and global change. *Coastal Environments and Global Change*, 1–27.

Mitsch, W. J., Day, J. W., Zhang, L., & Lane, R. R. (2005). Nitrate-nitrogen retention in wetlands in the Mississippi River Basin. *Ecological Engineering*, *24*(4), 267–278.

Mitsch, W. J., Zhang, L., Stefanik, K. C., Nahlik, A. M., Anderson, C. J., Bernal, B., Hernandez, M., & Song, K. (2012). Creating wetlands: Primary succession, water quality changes, and self-design over 15 years. *Bioscience*, *62*(3), 237–250.

Nixon, S. W., Ammerman, J. W., Atkinson, L. P., Berounsky, V. M., Billen, G., Boicourt, W. C., Boynton, W. R., Church, T. M., Ditoro, D. M., & Elmgren, R. (1996). The fate of nitrogen and phosphorus at the land-sea margin of the North Atlantic Ocean. *Biogeochemistry*, *35*(1), 141–180.

Pilegaard, K. (2013). Processes regulating nitric oxide emissions from soils. *Philosophical Transactions of the Royal Society B: Biological Sciences*, *368*(1621), 20130126.

Post, W. M., Pastor, J., Zinke, P. J., & Stangenberger, A. G. (1985). Global patterns of soil nitrogen storage. *Nature*, *317*(6038), 613–616.

Puckett, L. J. (1994). *Nonpoint and point sources of nitrogen in major watersheds of the United States* (Vol. 94, Issue 4001). US Geological Survey.

Reading, M. J., Santos, I. R., Maher, D. T., Jeffrey, L. C., & Tait, D. R. (2017). Shifting nitrous oxide source/sink behaviour in a subtropical estuary revealed by automated time series observations. *Estuarine, Coastal and Shelf Science*, *194*, 66–76.

Reading, M. J., Tait, D. R., Maher, D. T., Jeffrey, L. C., Looman, A., Holloway, C., Shishaye, H. A., Barron, S., & Santos, I. R. (2020). Land use drives nitrous oxide dynamics in estuaries on regional and global scales. *Limnology and Oceanography*, *65*(8), 1903–1920.

Reef, R., Feller, I. C., & Lovelock, C. E. (2010). Nutrition of mangroves. *Tree Physiology*, *30*(9), 1148–1160.

Rosentreter, J. A., Al-Haj, A. N., Fulweiler, R. W., & Williamson, P. (2021). Methane and nitrous oxide emissions complicate coastal blue carbon assessments. *Global Biogeochemical Cycles*, *35*(2), e2020GB006858.

Ryder, D., Burns, A., Veal, R., Schmidt, J., Robertson, M., Stewart, M., & Osborne, M. (2012). Coffs creek estuary coastal zone management plan literature and information review. *Heritage. Coffs Harbour City Council, Coffs Harbour, NSW*.

Sadat-Noori, M., Santos, I. R., Tait, D. R., Reading, M. J., & Sanders, C. J. (2017). High porewater exchange in a mangrove-dominated estuary revealed from short-lived radium isotopes. *Journal of Hydrology*, *553*, 188-198.

Sanders, C. J., Santos, I. R., Maher, D. T., Breithaupt, J. L., Smoak, J. M., Ketterer, M., Call, M., Sanders, L., & Eyre, B. D. (2016). Examining 239+ 240Pu, 210Pb and historical events to determine carbon, nitrogen and phosphorus burial in mangrove sediments of Moreton Bay, Australia. *Journal of Environmental Radioactivity*, *151*, 623–629.

Santos, I. R., de Weys, J., Tait, D. R., & Eyre, B. D. (2013). The contribution of groundwater discharge to nutrient exports from a coastal catchment: Post-flood seepage increases estuarine N/P ratios. *Estuaries and Coasts*, *36*(1), 56–73.

Santos, I. R. S., Burnett, W. C., Chanton, J., Mwashote, B., Suryaputra, I. G., & Dittmar, T. (2008). Nutrient biogeochemistry in a Gulf of Mexico subterranean estuary and groundwater-derived fluxes to the coastal ocean. *Limnology and Oceanography*, *53*(2), 705–718.

Scott, D. T., Keim, R. F., Edwards, B. L., Jones, C. N., & Kroes, D. E. (2014). Floodplain biogeochemical processing of floodwaters in the Atchafalaya River Basin during the Mississippi River flood of 2011. *Journal of Geophysical Research: Biogeosciences*, *119*(4), 537–546.

Sinha, E., Michalak, A. M., & Balaji, V. (2017). Eutrophication will increase during the 21st century as a result of precipitation changes. *Science*, *357*(6349), 405–408.

Tait, D. R., Maher, D. T., Sanders, C. J., & Santos, I. R. (2017). Radium-derived porewater exchange and dissolved N and P fluxes in mangroves. *Geochimica et Cosmochimica Acta*, *200*, 295–309.

Van Meter, K. J., Basu, N. B., Veenstra, J. J., & Burras, C. L. (2016). The nitrogen legacy: Emerging evidence of nitrogen accumulation in anthropogenic landscapes. *Environmental Research Letters*, *11*(3), 035014.

Venkiteswaran, J. J., Rosamond, M. S., & Schiff, S. L. (2014). Nonlinear response of riverine N2O fluxes to oxygen and temperature. *Environmental Science & Technology*, *48*(3), 1566–1573.

Wadnerkar, P. D., Andrews, L., Wong, W. W., Chen, X., Correa, R. E., White, S., Cook, P. L., Sanders, C. J., & Santos, I. R. (2021). Land use and episodic rainfall as drivers of nitrogen exports in subtropical rivers: Insights from δ15N-NO3−, δ18O-NO3− and 222Rn. *Science of the Total Environment*, *758*, 143669.

Wadnerkar, P. D., Andrews, L., Wong, W.-W., Chen, X., Correa, R. E., White, S., Cook, P., Sanders, C., & Santos, I. R. (2020). *The Runoff Carrying Capacity of Coffs Coast Estuaries*. National Marine Science Centre, Southern Cross University, Coffs Harbour ….

Wadnerkar, P. D., Batsaikhan, B., Conrad, S. R., Davis, K., Correa, R. E., Holloway, C., White, S. A., Sanders, C. J., & Santos, I. R. (2021). Contrasting radium-derived groundwater exchange and nutrient lateral fluxes in a natural mangrove versus an artificial canal. *Estuaries and Coasts*, *44*(1), 123–136.

Wadnerkar, P. D., Santos, I. R., Looman, A., Sanders, C. J., White, S., Tucker, J. P., & Holloway, C. (2019). Significant nitrate attenuation in a mangrove-fringed estuary during a flood-chase experiment. *Environmental Pollution*, *253*, 1000–1008.

Wadnerkar, P. D., White, S. A., Conrad, S. R., Morris, S. S., -, R. L., Holloway, C., Sanders, C. J., & Santos, I. R. (2021). Improving Water Quality Downstream of Protected Cropping Operations (Hothouses). *National Marine Science Centre, Southern Cross University, Coffs Harbour, NSW*.

Wang, W.-Q., Zeng, C.-S., Zhong, C.-Q., & Tong, C. (2010). Effect of human disturbance on ecological stoichiometry characteristics of soil carbon, nitrogen and phosphorus in Minjiang River estuarine wetland. *Huan Jing Ke Xue= Huanjing Kexue*, *31*(10), 2411–2416.

Wang, X., Wang, W., & Tong, C. (2016). A review on impact of typhoons and hurricanes on coastal wetland ecosystems. *Acta Ecologica Sinica*, *36*(1), 23–29.

Welti, N., Hayes, M., & Lockington, D. (2017). Seasonal nitrous oxide and methane emissions across a subtropical estuarine salinity gradient. *Biogeochemistry*, *132*(1–2), 55–69.

White, S. A., Conrad, S. R., Woodrow, R. L., Tucker, J. P., Wong, W. W., Cook, P. M., Sanders, C. J., Wadnerkar, P. D., Davis, K. L., & Holloway, C. J. (2020). Nutrient transport and sources in headwater streams surrounded by intensive horticulture. *Coffs Harbour City Council*, *57*.

White, S. A., Conrad, S. R., Woodrow, R. L., Tucker, J. P., Wong, W.-W., Cook, P. M., Sanders, C. J., Wadnerkar, P. D., Davis, K. L., & Holloway, C. J. (2021a). Natural attenuation of large anthropogenic nitrate loads in a subtropical stream revealed by δ15N and δ18O. *Journal of Hydrology*, *598*, 126077.

White, S. A., Santos, I. R., Conrad, S. R., Sanders, C. J., & Hessey, S. (2021b). Large aquatic nitrous oxide emissions downstream of intensive horticulture driven by rain events. *Journal of Hydrology*, *596*, 126066.

White, S. A., Santos, I. R., & Hessey, S. (2018). Nitrate loads in sub-tropical headwater streams driven by intensive horticulture. *Environmental Pollution*, *243*, 1036–1046.

Wong, W. W., Grace, M. R., Cartwright, I., Cardenas, M. B., Zamora, P. B., & Cook, P. L. (2013). Dynamics of groundwater-derived nitrate and nitrous oxide in a tidal estuary from radon mass balance modeling. *Limnology and Oceanography*, *58*(5), 1689–1706.

Wong, W. W., Pottage, J., Warry, F. Y., Reich, P., Roberts, K. L., Grace, M. R., & Cook, P. L. (2018). Stable isotopes of nitrate reveal different nitrogen processing mechanisms in streams across a land use gradient during wet and dry periods. *Biogeosciences*, *15*(13), 3953–3965.

Woodrow, R. L. (2021). Water parameters, nutrient, and gas samples in the Coffs Creek estuary, 2017-2018. PANGAEA.

Woodrow, R. L., White, S. A., Sanders, C. J., Holloway, C. J., Wadnerkar, P. D., Conrad, S. R., Davis, K. L., & Santos, I. R. (2021). Nitrous oxide hot moments and cold spots in a subtropical estuary: Floods and mangroves. *Estuarine, Coastal and Shelf Science*.

Wrage, N., Velthof, G. L., Van Beusichem, M. L., & Oenema, O. (2001). Role of nitrifier denitrification in the production of nitrous oxide. *Soil Biology and Biochemistry*, *33*(12–13), 1723–1732.

Zhang, Y., Ji, G., Wang, C., Zhang, X., & Xu, M. (2019). Importance of denitrification driven by the relative abundances of microbial communities in coastal wetlands. *Environmental Pollution*, *244*, 47–54.